IEEE Access
Multidisciplinary ⋮ Rapid Review ⋮ Open Access Journal

Received 1 December 2022, accepted 30 December 2022, date of publication 5 January 2023, date of current version 10 January 2023.

Digital Object Identifier 10.1109/ACCESS.2023.3234301

RESEARCH ARTICLE

Data-Driven Capacity Estimation of Li-Ion Batteries Using Constant Current Charging at Various Ambient Temperatures

MINJUN PARK, YOUNGBIN SONG, SHINA PARK, AND SANG WOO KIM, (Member, IEEE)
Department of Electrical Engineering, Pohang University of Science and Technology, Pohang 37673, South Korea

Corresponding author: Sang Woo Kim (swkim@postech.edu)

This work was supported by the National Research Foundation of Korea (NRF) funded by the Korean Government (MSIT) under Grant NRF-2021R1A2C2009966.

ABSTRACT The use of mobile devices, such as drones and electric vehicles, has rapidly increased in recent years. This has necessitated estimating the capacity of lithium-ion batteries in various situations. In this study, a capacity estimation algorithm using multilayer perceptron under different aging states and ambient temperature is proposed. The proposed algorithm estimates the capacity using charging time, voltage, and surface temperature, which can be measured during constant-current charging. Particularly, the surface temperature represents the state of battery differently than voltage. Therefore, the problem that the existing algorithm required a state of charge estimation was addressed, and the size of the neural network was significantly reduced. Using experimental data to validate the proposed algorithm, it was confirmed that the capacity was well estimated with a mean absolute error of 0.38% and a maximum error of 0.83%.

INDEX TERMS Li-ion battery, capacity, ambient temperature, surface temperature, machine learning, multilayer perceptron.

I. INTRODUCTION

A lithium-ion (Li-ion) battery has higher energy and power densities than other batteries. Therefore, it is used in various fields. This Li-ion battery degrades not only under natural operating conditions, such as cycle aging and calendar aging, but also in abnormal operating conditions, such as overcurrent, overdischarge, and over-charge [1]. The range of mobile devices, such as electric vehicles (EVs) and drones, may only be accurately estimated if the decreasing capacity of a Li-ion battery is accurately estimated. Consequently, the mobile device may not reach the next charging station. In this case, the EV must be towed, or the drone will crash. Additionalyy, if the mobile device ignores the lower voltage limit and continues to discharge, the battery gets overdischarged. Overdischarging causes the battery to rapidly degrade, or, in severe cases, an internal short circuit may occur, leading to an explosion [2]. Therefore, evaluating the capacity of a Li-ion battery is important for its long and safe use.

Existing capacity-estimation algorithms can be broadly classified into three methods: direct assessment, adaptive, and data driven [3]. Direct assessment can estimate the capacity via Coulomb counting, open circuit voltage (OCV), and electromechanical impedance spectroscopy (EIS) experiments. A typical method of direct assessment is Coulomb counting, which measures the capacity of battery by integrating current while fully charging and discharging. Additionally, the decreased capacity of a Li-ion battery can be estimated using changes in the OCV curve or increases in EIS measurements. These methods require a specific environment and are typically implemented in a laboratory setting. The adaptive approach is a method for estimating capacity using Kalman filters, particle filters, and the least square method, all based on the battery equivalent-circuit model [4], [5], [6], [7]. These methods are advantageous because their algorithms are applicable in real situations, such as in EVs with acceleration (discharge) and regenerative brakes (charge). However, incorrect

The associate editor coordinating the review of this manuscript and approving it for publication was Wentao Fan.

model parameter lead to significant variation in the estimation accuracy. The data driven method can estimate the capacity using the data accumulated through experiments, without using the equivalent model. The capacity estimation methods via the data driven method can be divided into differential analysis and machine learning methods [8]. The differential analysis method estimates capacity by using characteristics that appear in the incremental capacity (IC) curve or differential voltage curve by differentiating the capacity-OCV relationship [9], [10], [11], [12], [13], [14], [15]. Machine learning is a method of estimating capacity by extracting features from data collected during constant current (CC) or constant voltage charging processes or directly learning data, such as measured voltage and current [16], [17], [18].

The above methods assume a room-temperature environment. However, in reality, there are various outdoor air temperature conditions depend on the season or region. Several studies have been conducted on the characteristics that change significantly at low temperatures [19], [20]. Due to the decreased mobility of ions in a battery and the increased resistance of the charge transfer process on an electrode's surface in a low-temperature environment, the internal resistance increases significantly [19]. Moreover, [20] demonstrated the change in the resistance of the charge transfer process with temperature, showing that the internal resistance increased exponentially. However, incorporating the aging state into battery modeling at low temperatures is highly challenging because the mutual influence and nonlinearity of each variable must be considered in the model. Therefore, developing a capacity estimation algorithm for Li-ion batteries that considers the ambient air temperature is easy using the data-driven method.

Few algorithms considering ambient air temperature have been reported [21], [22], [23], [24]. The algorithms proposed by [21] and [22] estimate the state of charge (SOC) under various ambient temperatures using an equivalent model that calibrate the effect of temperature. The authors of [23] selected eight features by analyzing the correlation among the 14 health features proposed. The selected features were compressed through principal component analysis, and the capacity was estimated using the relevance vector machine. On validation with the NASA PcoE dataset, the estimated result had an error of less than 5% under most conditions, but the capacity was erroneous with an estimation error of less than 10% at 4 $^{\circ}C$. The authors of [24] proposed a method for estimating capacity using an IC curve and analyzed the changes in the IC curve according to the aging state, the SOC of CC charging, and the ambient temperature. This study demonstrated the characteristics of the change in the specific peak of the IC curve depending on the initial SOC of charging and corrected the estimated capacity. Additionally, it has been shown that the capacity can be estimated using a specific peak value that is not affected by the ambient temperature. However, to extract the peak unaffected by the ambient temperature, charging must start at a low SOC. Consequently, the consideration of the ambient air temperature in the existing algorithm is at an early stage, and a study on estimating capacity under various ambient temperatures and charging conditions is insufficient.

Meanwhile, using the surface temperature of Li-ion batteries in our previous work [18], the capacity can be estimated with a low error under various outside temperature conditions. In this case, the multilayer perceptron (MLP) network becomes very complicated, making it difficult to implement in a battery management system. Furthermore, the current capacity of the battery must be known to use the initial SOC value as an input to the MLP network to estimate the battery capacity.

In this study, an algorithm is proposed to estimate the capacity of degraded Li-ion batteries if charging is started below a specific voltage under various outdoor temperature conditions. The proposed algorithm estimates the capacity through an MLP using data at a particular voltage during CC charging until the end of CC charging. As inputs to the MLP, the voltage curve, charging time, average ambient temperature, and surface temperature of the Li-ion battery ranging from a specific voltage point to the end of CC charging were selected. By selecting CC charging, the proposed algorithm can work at various charging strategies that contain CC charging phase. Additionally, various methods for inputting the surface temperature were proposed to compare the estimation accuracy. The algorithm with the best estimation performance could estimate the capacity with errors of mean absolute error (MAE) 0.38% and maximum error (ME) 0.83%. The primary contributions of this study are as follows:

1) An algorithm was proposed to estimate the capacity at various outdoor temperatures using the characteristics of the CC charging voltage and battery surface temperature.
2) Using the change in the surface temperature of the Li-ion battery, the feature related to SOC was found regardless of the outside temperature.
3) An algorithm for estimating capacity without an initial SOC was proposed.
4) An algorithm was proposed to estimate the capacity with high accuracy by comparing inputs obtained by various methods.
5) The proposed algorithm was verified under five temperature conditions of 5°C, 15°C, 25°C, 40°C, and 55°C.

II. CHARACTERISTICS OF CC CHARGING

A. CHARACTERISTICS OF VOLTAGE CURVE

The OCV-SOC relationship changes according to the degradation of the cathode and anode active materials [25]. This change in the OCV-SOC curve reveals the voltage of CC charging, at which the battery is charged at a low current rate. In this case, the effect of voltage drop due to internal resistance is small, and the voltage change due to a change in internal resistance can be ignored. The changes in OCV-SOC curves with respect to degradation have been analyzed in

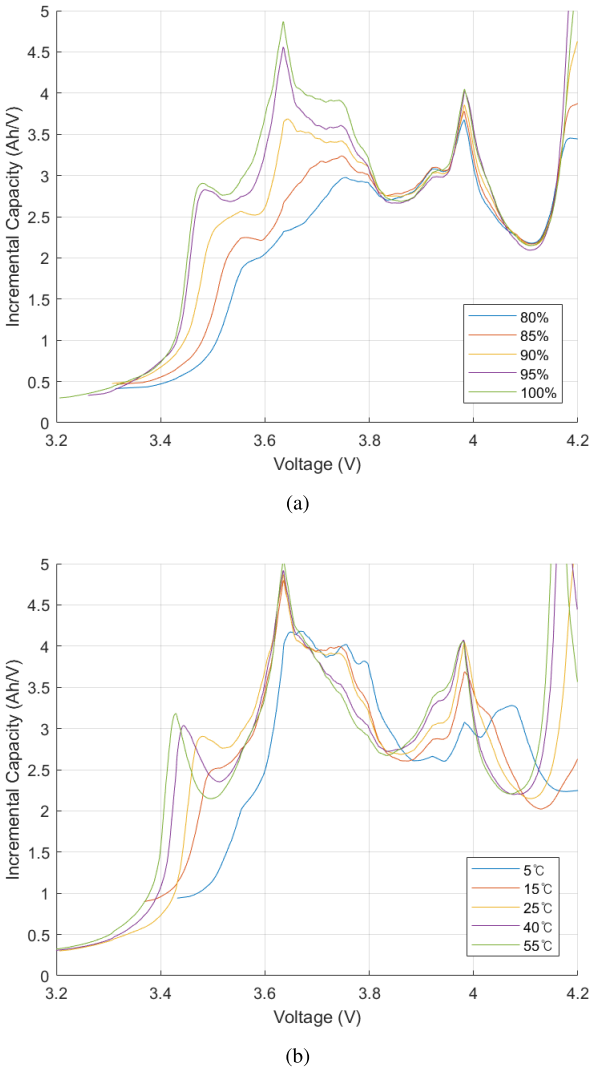

FIGURE 1. Change in Incremental capacity versus voltage. (a) Effect of degradation under a 25°C condition. (b) Effect of the ambient temperature of fresh battery.

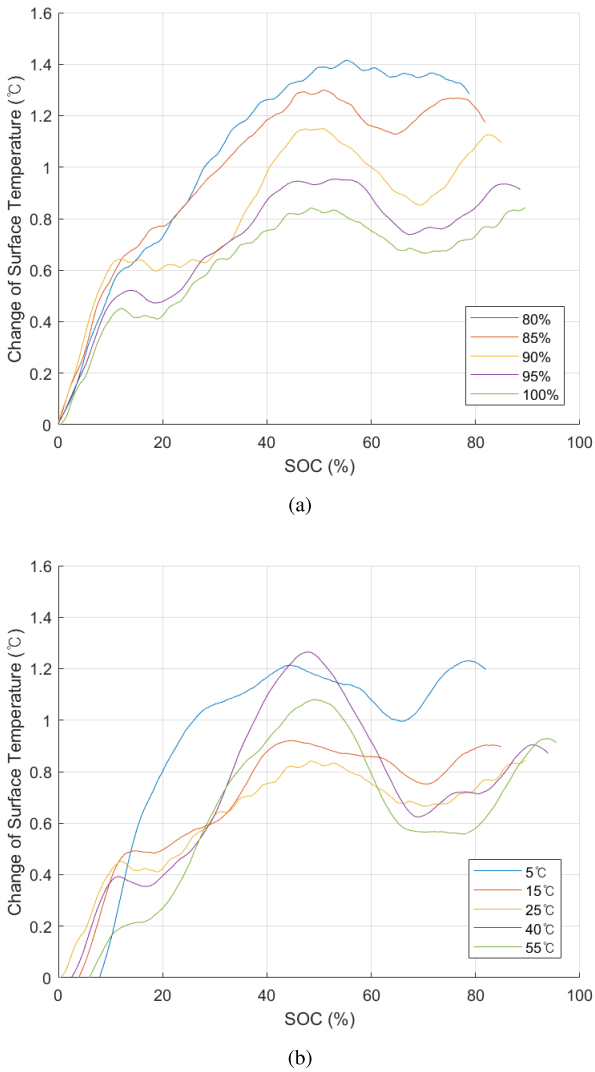

FIGURE 2. Change in surface temperature versus SOC (a) effect of degradation under 25°C condition, (b) effect of ambient temperature of fresh battery.

several studies [10], [24]. Existing methods estimate the capacity using features such as the peak or the valley of the IC curve. These peaks and valleys are proportional to the capacity, as shown in Fig. 1. Therefore, the capacity can be estimated at room temperature by measuring the size of the peak near 4 V. However, in the case of a low ambient temperature, the size of these peaks changes significantly (Fig. 1(b)), making it difficult to distinguish between the effects of aging and those of the low ambient temperature. Therefore, estimating the capacity by dividing the two effects is difficult and requires a complex network.

B. CHARACTERISTICS OF SURFACE TEMPERATURE

The surface temperature of the Li-ion battery is related to this heat generation. This heat generation can be expressed as the sum of the irreversible joule heat and the reversible reaction heat, as in (1).

$$HeatGeneration = IV_{ov} + IT\frac{\partial V_{oc}}{\partial T} \tag{1}$$

V_{ov} shows a voltage drop caused by internal resistance and V_{oc} represents the OCV. The joule heat can be expressed as the product of current and V_{ov}, whereas the reaction heat is defined as the product of current, temperature, and $\frac{\partial V_{oc}}{\partial T}$ due to the endothermic and exothermic chemical reactions in the Li-ion battery. This joule heat characteristcs is shown in common Li-ion battery [26]. When charging with a low current, due to the decrease in V_{oc} at a low current, the effect of the reaction heat is more dominant than the effect of joule heat. Additionally, $\frac{\partial V_{oc}}{\partial T}$ has a maximum value at 50% SOC, and an inflection point can be observed at 70% SOC. Due to these characteristics, identifiable issues can be observed even at the surface temperature of the Li-ion battery (Fig. 2). Therefore, information about the SOC at different points can

be indirectly obtained using the surface temperature. Due to necessity of this SOC information for calculating capacity, a capacity evaluation can be improved.

III. SOH ESTIMATION ALGORITHM

A. NO SURFACE TEMPERATURE METHOD

The existing algorithm presented in [18] estimates the battery capacity when charging is started at initial SOC but does not consider ambient temperature changes. To account for the temperature change in this algorithm, the capacity was estimated by adding the average surface temperature to the existing inputs, such as the initial SOC, charging time, and charging voltage curve. The number of input nodes configured in this case was 103. The number of hidden layers and nodes in each layer was changed and compared to determine the structure with the highest estimation performance. Therefore, the optimized structure required a significant number of multiplication operations. This structure is too large to be implemented in a battery management system with low computational capabilities.

B. PROPOSED METHOD

In the case of the previous algorithm, the complexity of the neural network increases when a broad range of initial SOC cases are considered. During CC charging, the data from the specific voltage point to the end of the CC charging point were selected to simplify the NN. IC curves and surface temperature curves in various cases were plotted to select a specific voltage point (Fig. 3). After approximately 3.9 V, the peak of the IC (Fig. 3(a)) and the inflection point (Fig. 3(b)) can be observed. Therefore, the capacity was estimated using the data measured during CC charging in the voltage range of 3.9 V-4.2 V. The measured data comprises the voltage, ambient temperature, surface temperature, and period of the selected range. The voltage curve was sampled at 100 points at equal intervals. An average of the ambient temperature is employed because the ambient temperature is approximately constant. The charging time in seconds was divided by 1,000 for scaling. In the case of surface temperature, we propose five input methods and compare the estimation precision of each method. The first method estimates the capacity without considering the surface temperature. The second method uses the average surface temperature, and the third uses 100 sampled points, similar to voltage sampling. In the fourth method, the initial temperature is subtracted, as shown in (2), to exclude the influence of the ambient temperature. The last method uses the rate of change in surface temperature, as shown in (3), so that the change in heat generation relative to phase change can be directly reflected.

$$T_{surf,0}(k) = T_{surf}(k) - T_{surf}(0) \tag{2}$$

$$T_{surf,del}(k) = 500(T_{surf}(k) - T_{surf}(k-1)) \tag{3}$$

In the above equation, $T_{surf}(k)$ represents a value obtained by sampling 100 points at equal intervals. Moreover, the scale is adjusted by multiplying by 500. This constant was arbitrarily

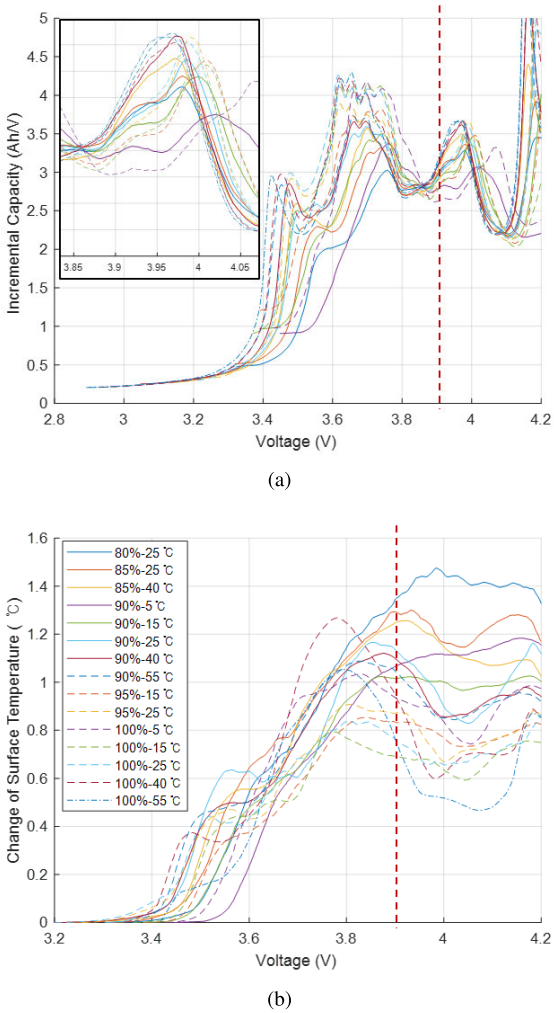

FIGURE 3. Incremental capacity and change in surface temperature in various conditions. (a) Incremental capacity. (b) Change in surface temperature.

selected. By configuring the inputs as above, the number of input nodes for the first and second NNs was 102 and 103, respectively, and the number of input nodes for the third, fourth, and fifth NNs was 202.

IV. MULTILAYER PERCEPTRON

The structure of neural network used for machine learning has various structures such as MLP, recurrent neural network (RNN), and convolutional neural network (CNN). Particularly, the RNN is suitable for processing time-series data, but it specializes in recognizing input patterns such as those in natural language processing. The CNN structure is suitable for extracting local characteristics from inputs through kernel and pooling layer. However, the CC charging curve and the surface temperature of the Li-ion battery represent different characteristics in each part. Therefore, the ability of CNN to extract characteristics from the local part is inappropriate. It can also be confirmed by a previous study [18] that the MLP structure shows a lower estimation error than the

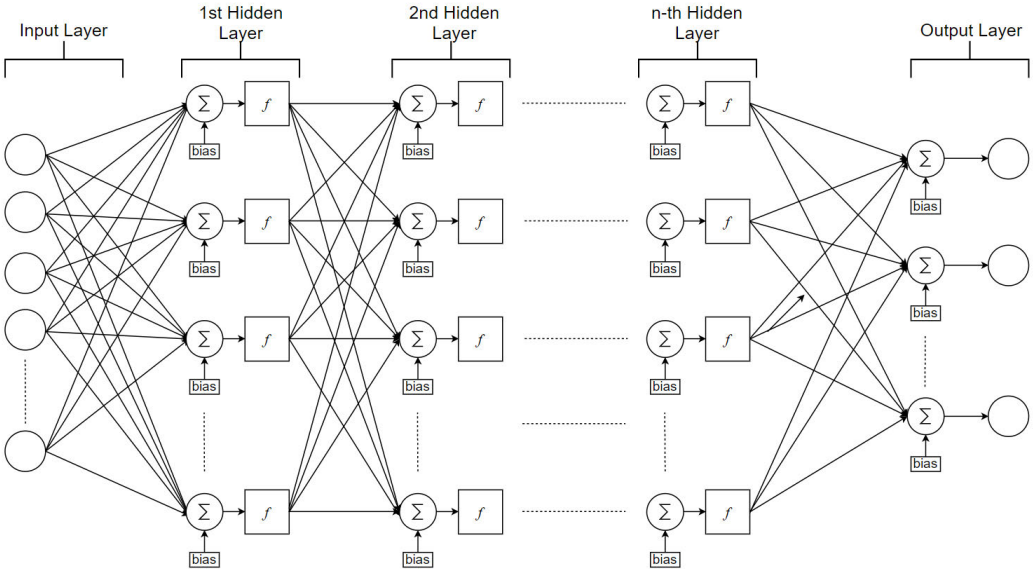

FIGURE 4. Structure of basic multilayer perceptron neural network.

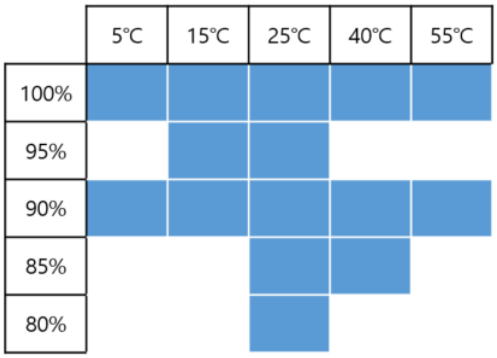

FIGURE 5. Conducted experiment conditions.

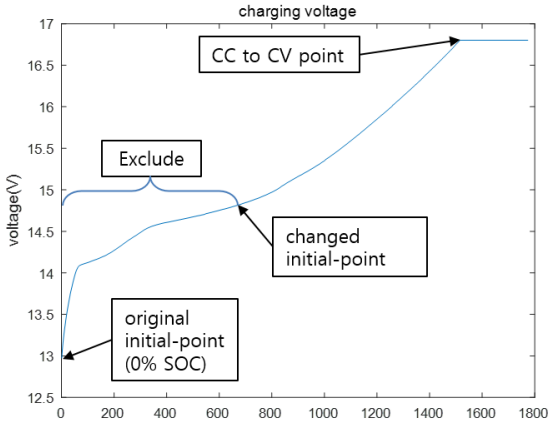

FIGURE 6. Data removal for the no surface temperature method.

CNN structure in the capacity estimation of a Li-ion battery. Therefore, in this study, the capacity was estimated using the MLP structure.

The MLP structure consists of an input layer, several hidden layers, and an output layer, and all layers are fully interconnected (Fig. 4). In this study, the number of hidden layers and the number of nodes in each hidden layer are determined by comparing estimation accuracies.

V. EXPERIMENT AND DATASET CONFIGURATION

Experiments were performed at ambient temperature and with aging under various conditions to validate the proposed methods. Three cells of Samsung INR18650-29E battery were used in the experiment, and the experimental data were obtained under limited conditions to reduce the experiment time. The conditions under which the experiment was conducted are depicted in Fig. 5.

In each aging state, a capacity of $25°C$ was measured. Subsequently, after a sufficient rest time at each temperature, the battery was discharged to the lower voltage limit at 0.2C, and the charging voltage was measured via standard charging. Afterward, all characteristic tests were completed in the corresponding aging state, and the accelerated aging process was performed by repeating CC charging and CC discharging until the next aging state. The data collected in this case consisted of three cells and 15 temperature-aging experimental points, totaling 45 data. Among these data, cells #1 and #2 were used as training sets to optimize the five proposed methods. In the case of the validation set, 100%-$40°C$, 100%-$15°C$, 95%-$25°C$, 90%-$55°C$, 90%-$5°C$, 90%-$5°C$, and 85%-$25°C$ cases of cell #3 were selected, and the remaining cases were used as test sets. Additionally, the estimated performance of the algorithm was compared using three-fold validation. During the three-fold validation, the validation and test sets were separated with the same combination.

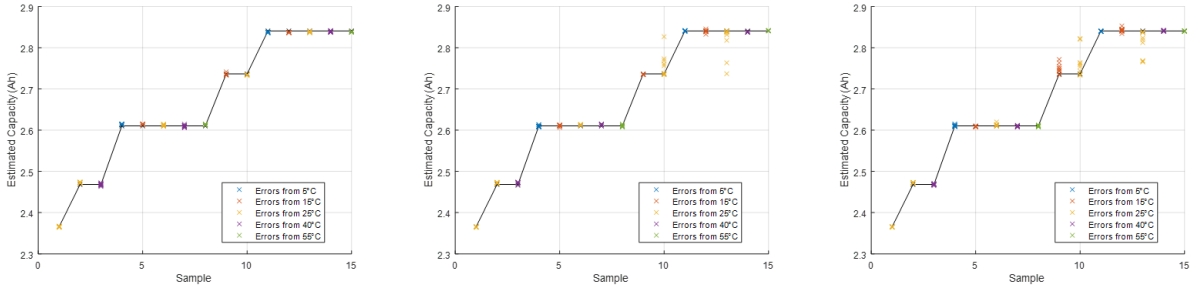

(a) (b) (c)

FIGURE 7. Estimation result of the no surface temperature method (a) 1792 nodes/layer and five hidden layers, (b) 1536 nodes/layer and five hidden layers, (c) 1792 nodes/layer and four hidden layers.

TABLE 1. Optimization result of each proposed method. Selected structures are shown in bold.

No T_{surf}			$T_{surf,avg}$			T_{surf}			$T_{surf,0}$			$T_{surf,del}$		
MLP	Test accuracy		MLP	Test accuracy		MLP	Test accuracy		MLP	Test accuracy		MLP	Test accuracy	
structure	MAE	ME	structure	MAE	ME	structure	MAE	ME	structure	MAE	ME	structure	MAE	ME
512/4	0.8359	4.6045	192/3	0.4700	2.3037	768/1	1.7087	5.5098	128/5	0.4012	2.3957	192/3	0.4700	2.3037
768/4	0.7163	4.7881	**256/3**	0.2269	0.8343	**1024/1**	1.6005	5.3685	**192/5**	0.1465	0.3713	**256/3**	0.2269	0.8343
1024/4	0.7692	4.3645	384/3	0.3103	1.4519	1280/1	2.9157	6.6346	256/5	0.3841	1.8542	384/3	0.3103	1.4819
768/3	0.8657	4.5912	256/2	0.8704	3.0868	1024/2	2.5457	7.5646	192/4	0.3470	1.6134	256/2	0.8704	3.0868
768/5	0.8483	4.6908	256/4	0.2253	0.8105				192/6	0.4897	3.1392	256/4	0.2253	0.8105

Because the data set used in the previous study was arbitrarily set at the starting point of charging, it is necessary to generate additional data from the given experimental data. As shown in Fig. 6, the length of the removed section was set to 0%, 5%, 10%, …, and 90% of the total CC section, generating 19 data points from one CCCV charging dataset. Among these data, the data from batteries #1 and #2 were used as the training sets, and the data from battery #3 were used as the validation and test sets. In this case, out of the 19 data points generated by a single CC charge, nine were randomly selected and used as the validation set, and the other ten were used as the test set.

VI. RESULT AND DISCUSSION

Using the data set configured in the previous section, the structure of the MLP was optimized for each case, and the estimation results were compared using MAE and ME. The equations for obtaining these indicators are as follows:

$$MAE = E(\frac{|Q_{true} - Q_{est.}|}{Q_{true}}) \times 100(\%) \quad (4)$$

$$ME = max(\frac{|Q_{true} - Q_{est.}|}{Q_{true}}) \times 100(\%) \quad (5)$$

The estimation results are organized in the following order: First, the optimization result of NN is shown. Second, the three-fold validation results for the proposed voltage range are shown. Finally, the three-fold validation results for different voltage ranges are presented.

A. OPTIMIZATION RESULT

1) No surface temperature method
Fig. 7 shows the estimation results of the optimized MLP structure using the previous study-based method. In this case, the estimation results are significantly high (Fig. 7(a)). However, a considerably high computational load was required because of the 1792 nodes per layer and five hidden layers. Additioinally a significant error occurs when the number of nodes per layer (Fig. 7(c)), or the number of layers is reduced (Fig. 7(d)) and even under slight reduction in MLP structures. Therefore, reducing computational load using the previous method is difficult.

2) Proposed method
In the five proposed methods, optimization was performed by changing the numbers of nodes per layer and hidden layers to determine the point where the local minima appear. Table 1 summarizes the optimization results of all the methods. In this table, the MLP structure is expressed in the order of ''nodes per layer'' and ''hidden layers.''

B. THREE-FOLD VALIDATION

The estimated performance of each optimized method was compared through three-fold validation. In this case, a voltage corresponding to 3.9 V has been distributed between 43% and 60% SOC. When T_{surf} and $T_{surf,avg}$ were used for estimation, the MAE significantly increased compared to when T_{surf} was not used, and the ME also significantly increased. By contrast, when $T_{surf,0}$ and $T_{surf,del}$ were used, high estimation results were shown in Fig. 9, except for the network trained with B2 and B3. Even after training with B2 and B3, a particular sample showed approximately 4% error, resulting in a significant ME but only approximately 1% error in MAE. In this case, the number of product operations among the hidden

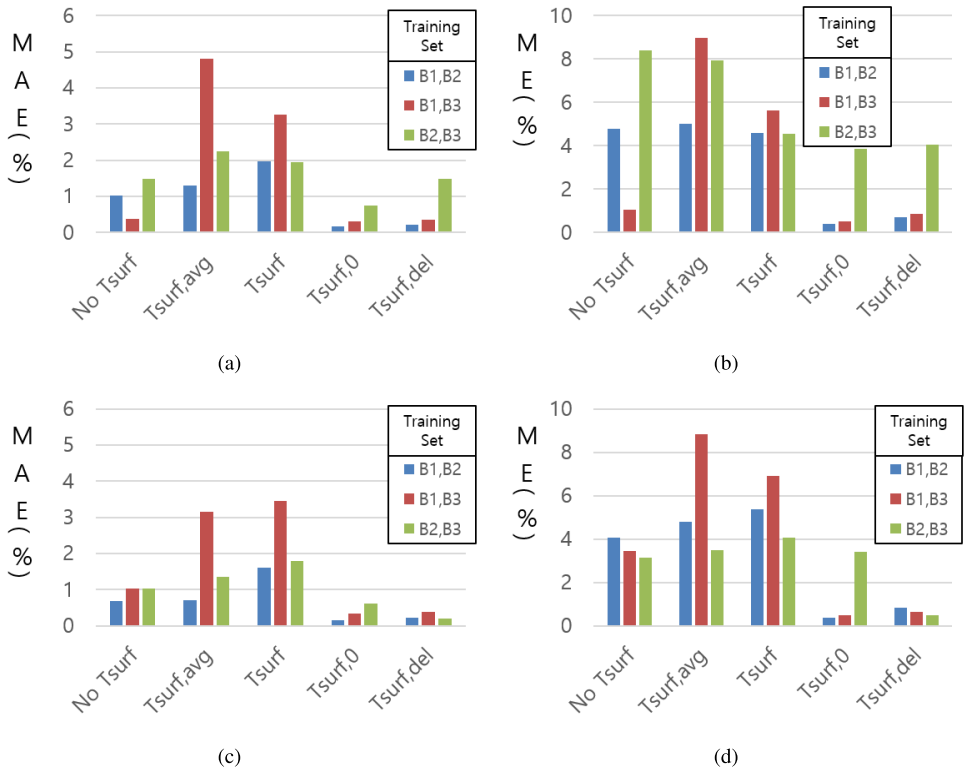

FIGURE 8. Three-fold validation results of the proposed method with 3.9-4.2 V range. (a) MAE of the validation set, (b) ME of the validation set, (c) MAE of the test set, (d) ME of the test set.

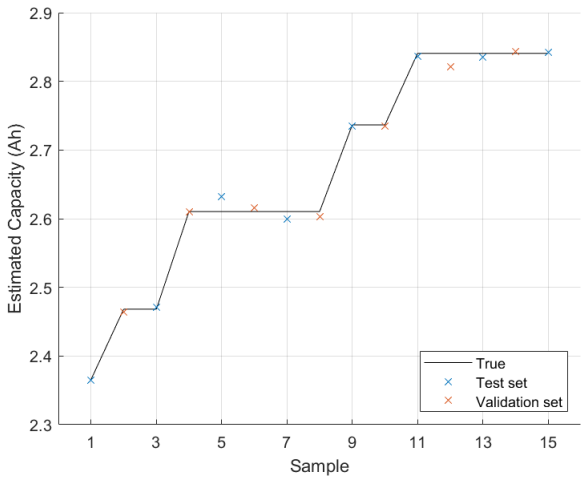

FIGURE 9. Result of proposed capacity estimation algorithm in case of $T_{surf,del}$, 3.9-4.2 V range and trained using B1, B2.

layers of $T_{surf,0}$ and $T_{surf,del}$ is 4×192^2 (approximately 150k) and 2×256^2 (approximately 130k), respectively. Hence, the no surface temperature method, which is similar to previous work [18], consists of 1792 nodes per layer and five hidden layers. This structure needs to perform 12.8M multiplications among its hidden layers. This difference in the number of multiplications is due to additional information on the surface temperature.

C. DIFFERENT VOLTAGE THRESHOLD

To compare the estimation accuracy in different voltage ranges, additional verification was conducted in the 3.85-4.2 V and 3.95-4.2 V ranges. The SOC corresponding to 3.95 V was distributed in the range of 50%-66%, and the SOC corresponding to 3.85 V was distributed in the range of 37%-55%.

1) 3.95-4.2 V range
Fig. 10 shows the estimation results obtained when the algorithm was constructed based on the 3.95-4.2 V range. In this case, because a narrower range of data was input, low estimation accuracy was demonstrated owing to the lack of input information. The ME of the validation and test sets increased overall, and the number of samples with large errors increased, resulting in a slight increase in MAEs.

2) 3.85-4.2 V range
Fig. 11 shows the estimation results when the algorithms are constructed based on the 3.85-4.2 V range. In this case, because a wider range of data was input, the input information was abundant, showing a high estimation accuracy. Particularly, when $T_{surf,0}$ was used, low estimation errors were observed in both the validation and test sets. Meanwhile, to sample from a voltage corresponding to 3.85 V, it is necessary to start charging at a lower SOC. When implementing an actual algorithm, an appropriate voltage criterion should be chosen considering this trade-off relationship.

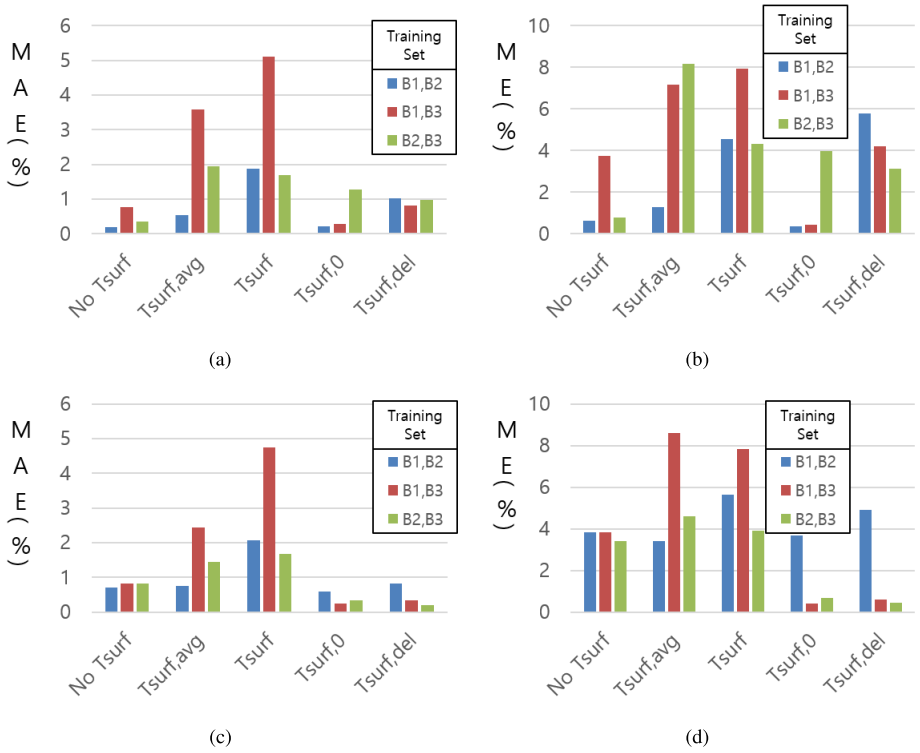

FIGURE 10. Three-fold validation results of the proposed method with 3.95-4.2 V range (a) MAE of the validation set, (b) ME of the validation set, (c) MAE of the test set, (d) ME of the test set.

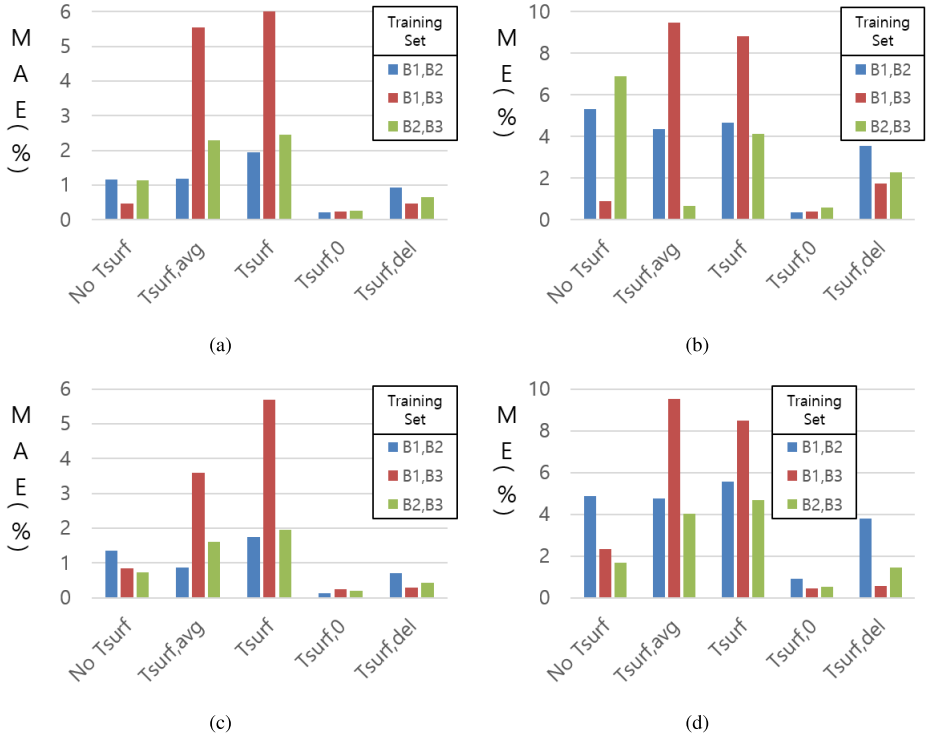

FIGURE 11. Three-fold validation results of the proposed method with 3.85-4.2 V range (a) MAE of the validation set, (b) ME of the validation set, (c) MAE of the test set, (d) ME of the test set.

VII. CONCLUSION

In this study, a capacity estimation algorithm was proposed using the CC charging curve of Li-ion batteries, considering changes in ambient temperature. CC charging of Li-ion batteries shows characteristics in the voltage curve and surface temperature. The proposed algorithm estimated the capacity

using measured data between 3.9 and 4.2 V. By comparing various surface temperature input methods, the method with highest estimation performance was selected. Comparing the optimization results and the estimation performance of the proposed methods shows that $T_{surf,0}$ or $T_{surf,del}$ increased estimation performance. Additionally, the computation amount of the proposed method was significantly less than that of the existing method, and the performance of the proposed algorithm was estimated with low error rates of MAE 0.38% and ME 0.83%. Particularly, the proposed algorithm verified the effectiveness of capacity estimation under various ambient temperature conditions that were not previously considered and showed that it could be used in various situations. It was demonstrated that the proposed capacity estimation algorithm is suitable for a battery management system, such as when charging an EV in cold regions. The data used in this study have limited aging points and cannot account for various charging currents and aging conditions; therefore, future studies could experiment with an algorithm to estimate the capacity under different conditions.

REFERENCES

[1] M. M. Kabir and D. E. Demirocak, "Degradation mechanisms in Li-ion batteries: A state-of-the-art review," *Int. J. Energy Res.*, vol. 41, no. 14, pp. 1963–1986, 2017.

[2] C. Wu, J. Sun, C. Zhu, Y. Ge, and Y. Zhao, "Research on overcharge and overdischarge effect on lithium-ion batteries," in *Proc. IEEE Vehicle Power Propuls. Conf. (VPPC)*, Oct. 2015, pp. 1–6.

[3] M. H. Lipu, M. Hannan, A. Hussain, M. Hoque, P. J. Ker, M. H. M. Saad, and A. Ayob, "A review of state of health and remaining useful life estimation methods for lithium-ion battery in electric vehicles: Challenges and recommendations," *J. Cleaner Prod.*, vol. 205, pp. 115–133, Dec. 2018.

[4] P. Shen, M. Ouyang, L. Lu, J. Li, and X. Feng, "The co-estimation of state of charge, state of health, and state of function for lithium-ion batteries in electric vehicles," *IEEE Trans. Veh. Technol.*, vol. 67, no. 1, pp. 92–103, Jan. 2017.

[5] Y. Gao, K. Liu, C. Zhu, X. Zhang, and D. Zhang, "Co-estimation of state-of-charge and state-of-health for lithium-ion batteries using an enhanced electrochemical model," *IEEE Trans. Ind. Electron.*, vol. 69, no. 3, pp. 2684–2696, Mar. 2022.

[6] X. Lai, W. Yi, Y. Cui, C. Qin, X. Han, T. Sun, L. Zhou, and Y. Zheng, "Capacity estimation of lithium-ion cells by combining model-based and data-driven methods based on a sequential extended Kalman filter," *Energy*, vol. 216, Feb. 2021, Art. no. 119233.

[7] L. Ling and Y. Wei, "State-of-charge and state-of-health estimation for lithium-ion batteries based on dual fractional-order extended Kalman filter and online parameter identification," *IEEE Access*, vol. 9, pp. 47588–47602, 2021.

[8] Y. Li, K. Liu, A. M. Foley, A. Zülke, M. Berecibar, E. Nanini-Maury, J. Van Mierlo, and H. E. Hoster, "Data-driven health estimation and lifetime prediction of lithium-ion batteries: A review," *Renew. Sustain. Energy Rev.*, vol. 113, Oct. 2019, Art. no. 109254.

[9] T. Goh, M. Park, M. Seo, J. G. Kim, and S. W. Kim, "Capacity estimation algorithm with a second-order differential voltage curve for Li-ion batteries with NMC cathodes," *Energy*, vol. 135, pp. 257–268, Sep. 2017.

[10] Y. Li, M. A. Monem, R. Gopalakrishnan, M. Berecibar, E. N. Maury, N. Omar, P. Bossche, and J. V. Mierlo, "A quick on-line state of health estimation method for Li-ion battery with incremental capacity curves processed by Gaussian filter," *J. Power Sources*, vol. 373, pp. 40–53, Jan. 2018.

[11] X. Bian, Z. Wei, J. He, F. Yan, and L. Liu, "A novel model-based voltage construction method for robust state-of-health estimation of lithium-ion batteries," *IEEE Trans. Ind. Electron.*, vol. 68, no. 12, pp. 12173–12184, Dec. 2021.

[12] Y. Zhang, Y. Liu, J. Wang, and T. Zhang, "State-of-health estimation for lithium-ion batteries by combining model-based incremental capacity analysis with support vector regression," *Energy*, vol. 239, Jan. 2022, Art. no. 121986.

[13] Z. Lyu, R. Gao, and X. Li, "A partial charging curve-based data-fusion-model method for capacity estimation of Li-ion battery," *J. Power Sources*, vol. 483, Jan. 2021, Art. no. 229131.

[14] T. Sun, B. Xu, Y. Cui, X. Feng, X. Han, and Y. Zheng, "A sequential capacity estimation for the lithium-ion batteries combining incremental capacity curve and discrete Arrhenius fading model," *J. Power Sources*, vol. 484, Feb. 2021, Art. no. 229248.

[15] C. Qian, B. Xu, L. Chang, B. Sun, Q. Feng, D. Yang, Y. Ren, and Z. Wang, "Convolutional neural network based capacity estimation using random segments of the charging curves for lithium-ion batteries," *Energy*, vol. 227, Jul. 2021, Art. no. 120333.

[16] M. Berecibar, F. Devriendt, M. Dubarry, I. Villarreal, N. Omar, W. Verbeke, and J. Van Mierlo, "Online state of health estimation on NMC cells based on predictive analytics," *J. Power Sources*, vol. 320, pp. 239–250, Jul. 2016.

[17] J. Meng, L. Cai, D.-I. Stroe, X. Huang, J. Peng, T. Liu, and R. Teodorescu, "An automatic weak learner formulation for lithium-ion battery state of health estimation," *IEEE Trans. Ind. Electron.*, vol. 69, no. 3, pp. 2659–2668, Mar. 2022.

[18] M. Park, M. Seo, Y. Song, and S. W. Kim, "Capacity estimation of Li-ion batteries using constant current charging voltage with multilayer perceptron," *IEEE Access*, vol. 8, pp. 180762–180772, 2020.

[19] J. Jaguemont, L. Boulon, and Y. Dubé, "A comprehensive review of lithium-ion batteries used in hybrid and electric vehicles at cold temperatures," *Appl. Energy*, vol. 164, pp. 99–114, Feb. 2016.

[20] S. S. Zhang, K. Xu, and T. R. Jow, "Electrochemical impedance study on the low temperature of Li-ion batteries," *Electrochimi. Acta*, vol. 49, no. 7, pp. 1057–1061, 2004.

[21] M. Seo, Y. Song, J. Kim, S. W. Paek, G.-H. Kim, and S. W. Kim, "Innovative lumped-battery model for state of charge estimation of lithium-ion batteries under various ambient temperatures," *Energy*, vol. 226, Jul. 2021, Art. no. 120301.

[22] R. Xiong, J. Wang, W. Shen, J. Tian, and H. Mu, "Co-estimation of state of charge and capacity for lithium-ion batteries with multi-stage model fusion method," *Engineering*, vol. 7, no. 10, pp. 1469–1482, Oct. 2021.

[23] P. Y. Guo, Z. Cheng, and L. Yang, "A data-driven remaining capacity estimation approach for lithium-ion batteries based on charging health feature extraction," *J. Power Sources*, vol. 412, pp. 442–450, Feb. 2019.

[24] B. Jiang, H. Dai, and X. Wei, "Incremental capacity analysis based adaptive capacity estimation for lithium-ion battery considering charging condition," *Appl. Energy*, vol. 269, Jul. 2020, Art. no. 115074.

[25] J. Tian, R. Xiong, W. Shen, and F. Sun, "Electrode ageing estimation and open circuit voltage reconstruction for lithium ion batteries," *Energy Storage Mater.*, vol. 37, pp. 283–295, May 2021.

[26] J. Marcicki and X. G. Yang, "Model-based estimation of reversible heat generation in lithium-ion cells," *J. Electrochemical Soc.*, vol. 161, no. 12, pp. A1794–A1800, 2014.

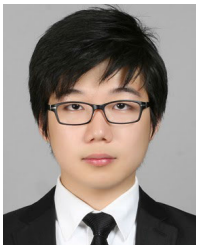

MINJUN PARK was born in Deagu, South Korea, in July 1989. He received the B.S. degree in electronic engineering from Kyungpook National University, Deagu, in 2014, and the M.S. degree in electrical engineering from the Pohang University of Science and Technology, Pohang, South Korea, in 2016, where he is currently pursuing the Ph.D. degree in electrical engineering.

His research interests include state estimation and remain useful life prediction of lithium-ion battery using deep learning.

YOUNGBIN SONG was born in Deagu, South Korea, in November 1992. He received the B.S. degree in electronic engineering from Kyungpook National University, Deagu, in 2018, and the M.S. degree in electrical engineering from the Pohang University of Science and Technology, Pohang, South Korea, in 2020, where he is currently pursuing the Ph.D. degree in electrical engineering.

His research interests include state estimation and modeling of lithium-ion battery using control and signal processing.

SHINA PARK was born in Seoul, South Korea, in July 1994. She received the B.S. degree in electrical and electronics engineering from Chung-Ang University, Seoul, in 2020, and the M.S. degree in electrical engineering from the Pohang University of Science and Technology, Pohang, South Korea, in 2022, where she is currently pursuing the Ph.D. degree in electrical engineering. Her research interests include state estimation and modeling of lithium-ion battery using control and signal processing.

SANG WOO KIM (Member, IEEE) was born in Pyeongtack, South Korea, in August 1961. He received the B.S., M.S., and Ph.D. degrees in control and instrumentation engineering from Seoul National University, Seoul, South Korea, in 1983, 1985, and 1990, respectively.

In 1992, he joined the Pohang University of Science and Technology, Pohang, South Korea, as an Assistant Professor, where he is currently a Full Professor with the Department of Electrical Engineering. In 1993, he was a Visiting Fellow with the Department of System Engineering, The Australian National University, Canberra, Australia. His research interests include optimal control, optimization algorithms, intelligent control, wireless communication, and process automation.